

Observations of terrestrial lighting at optical wavelengths by the photodiode detector on the FORTÉ satellite

M.W. Kirkland, D.M. Suszcynsky and R. Franz

Space and Atmospheric Sciences Group, Mail Stop D466, Los Alamos National Laboratory, Los Alamos, New Mexico, 87545.

J.L.L. Guillen and J.L. Green

Sensors and Electronics Department, Mail Stop 0972, Sandia National Laboratories, Albuquerque, New Mexico, 87185.

R.E. Spalding

System Assessment and Research Center 5900, Sandia National Laboratories, Mail Stop 0978, Albuquerque, NM 87185

Abstract

We present data from observations of terrestrial lightning from the FORTÉ satellite obtained during its first year of operation. A silicon photodiode detector records the intensity-time history of transient optical events occurring within its 80-degree circular field of view. This field of view corresponds to a circle on the Earth's surface having an approximate diameter of 1200 kilometers. Events having inferred powers between 10^8 and 10^{12} watts, and effective pulse widths of hundreds of microseconds, are observed. We present examples of the data, explain how the data is screened for false triggers, review the general statistics of peak irradiance, pulse width and energy associated with the data, and infer a median path length through lightning-producing clouds.

Introduction

Satellite-based observations of radio frequency (RF) and optical emissions from lightning have been occurring for over 30 years [Vorpahl *et al.*, 1970; Sparrow and Ney, 1971; Turman, 1977, 1978; Vonnegut *et al.*, 1983]. Optical emissions from terrestrial lightning were first detected from space by NASA's Orbiting Solar Observatory (OSO)-2 satellite in the mid-1960s. Since that time, additional optical observations of lightning have been made by the OSO, VELA, Defense Meteorological Satellite Program (DMSP) and Global Positioning System (GPS) series of satellites. The VELA, DMSP and GPS observations provided a time history of optical pulses produced by lightning. More recently, NASA has launched and operated optical imaging sensors (Optical Transient Detector and Lightning Imaging Sensor) in low Earth orbit to study terrestrial lightning. These imaging sensors provide the capability to determine the geographic location and peak amplitude of detected lightning events [e.g., Christian *et al.*, 1989].

The FORTÉ satellite was launched on 29 August 1998 into a nearly 825-km circular, 70-degree inclination orbit. This Department of Energy satellite carries optical and RF sensors and serves as an engineering test-bed for advanced sensor technologies to be carried on the next generation of nuclear test ban treaty-monitoring satellites. An additional benefit of this satellite is its superb ability to simultaneously monitor the optical and RF emissions of lightning activity on a global basis. In the first year of operation, over two million optical and RF events have been detected by the sensors on FORTÉ and an initial presentation of the RF data has been given by *Jacobson* [1998]. This paper will focus on data collected by one of the two optical sensors carried by FORTÉ – a silicon photodiode detector. This instrument records the amplitude time history of transient optical events within the field of view. We present examples of data obtained with this instrument along with a statistical overview of terrestrial lightning as observed from space.

Instrument

The FORTÉ satellite carries two instruments that comprise the Optical Lightning Subsystem (OLS). The Lightning Location System (LLS) employs a CCD array having an 80° field of view (FOV), a 10 Å passband filter centered on 777.4 nm, and the electronics necessary to trigger on transient optical events having pulse widths shorter than a few milliseconds. The LLS was designed to determine the 2-D geographic location of lightning events with 10-km accuracy. The other OLS instrument is the photodiode detector (PDD). The PDD consists of an unfiltered, single element silicon photodiode with one square centimeter of sensing area. The PDD is responsive to wavelengths from 400- to 1100-nm, with the peak response near 850-nm. A 6-inch long sunshade provides a circular 80° FOV to match that of the LLS. The PDD measures the intensity of incoming light in its FOV and triggers on impulsive events, providing the means to record the light-intensity time history of lightning flashes occurring within the FOV of the instrument. In this paper, we exclusively present data obtained with the PDD. A fully detailed description of the PDD will be given in a forthcoming paper that will address the entire OLS payload. In this present work, we describe only those elements of the PDD essential for understanding the data presented in this paper.

The PDD employs 12-bit sampling to provide an effective dynamic range spanning more than four orders of magnitude. The 12-bit sampling allows for a sign bit and 11 bits of resolution. The total dynamic range is piece-wise linear, with one half of the range provided by the least significant 10 bits. Two additional levels of compression are achieved with the remaining bit. The finest granularity in the PDD sensitivity is better than 10^{-5} watts meter². The analog PDD electronics continuously compensate for the slowly varying background signal to allow the full dynamic range to be used for transient signals. The background compensation rate can be set into one of four rate modes. The slowest compensation rate is typically employed when the satellite views a dark Earth. The fastest compensation rate is used for day/night terminator crossings, when the light level from the background scene changes rapidly.

The PDD also has four modes of operation: internal trigger mode, external trigger mode, slave mode and test mode. In this paper, we present only those data generated by internal triggers, so we only discuss that mode in this paper. However, we note that the external mode allows the PDD to be triggered by either the radio-frequency (RF) subsystem onboard FORTE, or by the LLS, but is essentially like the internal trigger mode. The slave mode allows the LLS to trigger the PDD, and a longer PDD time history is retained.

In the case of the internal trigger mode, the compensated photodiode signal is digitized every 15- μ s and inserted into a FIFO storage buffer. When 32 samples have been written into the FIFO buffer, subsequent samples are also compared with the trigger level. The trigger level is either set manually, or placed into a noise-riding mode. In the noise-riding mode, the trigger level is based upon the contemporary noise level calculation performed by the OLS processor once per second and is derived by simply taking the product of an adjustable multiplier (typically 5) and the calculated background rms noise level provided by the OLS processor. If the digitized signal level exceeds the trigger level for a predetermined number (0-31, typically 5) of samples, then a trigger is generated. This duration test typically rejects triggers due to the passage of energetic particles through the photodiode. Once a trigger is generated, another 96 samples are written into the FIFO buffer. An event message containing the 128 samples is then formatted, stored in the OLS memory and the PDD electronics are reset.

The time tag for the trigger is assigned based on the 2.098 MHz OLS clock, which is conditioned by a 1 Hz GPS-derived signal. We expect thermal variations and uncertainties in the OLS circuitry to introduce less than 25 μ s of variability into the assigned trigger time. The minimum inter-trigger delay is dictated by the requirement to acquire the 96 post-trigger samples, format the event message, reset the electronics and acquire 32 new samples. In practice we have found this inter-trigger delay to be about 4.4 milliseconds. This delay is sufficiently small enough to allow the PDD to capture sequences of cloud-ground lightning strokes within a flash, provided the trigger criteria are satisfied.

One caveat to the capture of stroke sequences within a flash is that the PDD will automatically temporarily disable itself until the next 1-Hz time hack if more than a specified number (usually 10) events are recorded within a specified time window (usually 40 milliseconds). This rate limit is imposed to avoid filling the OLS memory with a rapid succession of transient events that occur due to glint off of spacecraft or ocean surfaces, or from anomalous signals that may occur during day/night terminator crossings when the background scene is changing rapidly.

Data Reduction

During the period between launch and mid-July 1998, the PDD had detected some 435,000 events. Approximately 82% of these events were detected between 1800-0600 local time (LT) (i.e. “mostly night”), while the remaining events were detected between 0600-1800 LT (i.e. “mostly day”). No effort has been made to remove sampling biases incurred by some preferential operation of the PDD over a dark earth. However, an

attempt to operate the PDD without preference to local time has been made since March 1998. It is noteworthy that approximately one-half of the total number of PDD events reported in this paper have been recorded since 15 March 1998. Thus the disparity in the day/night detection ratio does heavily reflect the effect of a sunlit earth on the lightning-detection capabilities of the PDD, as opposed to attributing all of the disparity to sampling preferences.

We have examined the distribution of the measured peak irradiances from all PDD events, and also the waveforms of several thousands of events selected randomly from this distribution. We found a few percent of events to be due to energetic particles, which are recorded when the PDD is set into the internal trigger mode and the duration test is disabled or set to a small (< 5 samples) value. Particle signals are also occasionally captured by accident during slave mode triggers, but we note that slave mode triggers are generated by the LLS, and not by the passage of the particle through the photodiode. We also found a class of events whose waveforms exhibit a character more like noise (e.g. due to glint or instrument electronic noise) than the characteristic curve obtained from observations of lightning. A typical “noise” event is characterized by a highly oscillatory signal, having a rms amplitude that varies with the magnitude of the dc offset upon which the signal is superposed. We endeavored to flag the particle and noise-induced triggers in the PDD data set.

Figure 1 illustrates the three basic types of PDD waveforms. From left to right, the three panels in Figure 1 show (i) a typical signal obtained from an optical lightning emission, (ii) a typical slowly-varying (across the 1.9-ms record) signal classified as “noise-induced” and (iii) a typical signal classified as “due to energetic particle.” In future work we will closely scrutinize those curves obtained from optical lightning emissions (type (i)) to determine whether or not the sub-classification of these waveforms has any physical basis. A few of the type (ii) category signals, which change slowly across the 1.9-ms record, could actually be segments of slowly-changing, long-duration optical emissions from within the atmosphere, such as those generated by bolide-type objects entering the Earth’s atmosphere. We emphasize that this claim is unsubstantiated and point out that the noise curve shown in Figure 1 is not suspected of being such an event.

We endeavor to identify and remove from consideration the triggers attributed to energetic particles and noise. In the case of waveforms that exhibit the noise behavior described above, we impose a requirement that the maximum signal amplitude exceed the minimum signal amplitude by more than an order of magnitude. This requirement eliminates most of the type (ii) false triggers and removes approximately 38% of the entire data set. It is worth noting that this criterion was originally based on a review of thousands of PDD waveforms and that this criterion does not significantly affect the peak amplitude distribution of PDD events, as will be shown below.

In the case of false triggers generated by energetic particles, we are able to isolate these signals by first imposing the noise-rejection test above. We subsequently impose the requirement that the sampled signal not decrease in amplitude by more than a factor of two between successive samples. Moreover, amplitude drops by more than a factor of

two cannot occur more than 3 times within the first 100 μs following the trigger point. Further, the signal amplitude is not allowed to fall below the trigger level within 100 μs of the trigger point. This criterion removes approximately 5% of the entire data set. Most of these particle triggers occurred during the early portion of the mission when the duration test was set to low (< 5 samples) values.

After imposing these particle- and noise-rejection criteria, we are left with approximately 57% of the total number of PDD triggers obtained since launch. What now remains is a reduced population of events attributed to optical lightning emissions. This population of triggers will form the data set from which we derive our statistics and that we compare with previous observations of optical emissions from lightning. We will refer to the entire population of PDD triggers as the “unfiltered” population. The sub-population of down-selected events will be referred to as “filtered” events.

Prior to our discussion of these data, it should be noted that our filtered data set does contain those events that were triggered by lightning, but for which the compensation rate may have been too slow or too fast. In cases where the background intensity is increasing, but the compensation rate is too slow or too fast, the peak signal amplitudes will be artificially elevated or depressed respectively. In a rigorous treatment of the data, these effects would be identified and removed. Unfortunately it is not possible to discriminate against events for which the compensation rate was not ideal due to the possibility of mis-identifying those events that result from rapid, sequential re-triggering of the PDD on long duration, structured optical signals such as those seen in Figure 2.

Figure 3 shows two curves that represent the distribution of peak amplitudes for unfiltered events (dashed line), and for filtered events (solid line). The trailing (left) edge of the filtered event distribution shows a hard cut-off at approximately $3 \times 10^{-5} \text{ Wm}^{-2}$. This

Observations

As an introductory example, we refer to Figure 2 which shows a sequence of events on a common time axis that were recorded east of Hawaii at 08:37:55 UT on 8 October 1997. Each of the four curves shows structure. *Brook et al.* [1985] also noted structure in observations of trans-cloud optical lightning signals taken at an altitude of 20 km. They interpreted this structure as due to dart or stepped leader processes, or branching of the lightning channel. *Goodman et al.* [1988] have made similar interpretations of their above-cloud observations of lightning. The interpulse delay between successive events in Figure 2 is consistent with intra-cloud discharges, and one might interpret the finer structure as due to branching of the lightning channel. The task of studying the pulse shapes observed by the PDD and relating them to CG and IC events remains a future work. Prior to undertaking such a venture, it is necessary to understand the statistical nature of the data. Thus we now focus our attention on this aspect of our data for the remainder of this paper.

As described above, Figure 3 shows the peak amplitude distribution of PDD events. For comparison, the level of the optically bright events (superbolts) having optical powers $>$

10^{12} W that were observed by *Turman* [1977] are indicated. The VELA and DMSP optical data reported by *Turman* [1977,1978] are the only comparable (pulse time history) data from satellite-based observations of lightning emissions that are known to these authors to have been previously reported. The median peak optical irradiance observed by the PDD is about 1.3×10^{-4} W m⁻², corresponding to a peak optical power of 1×10^9 W. This median value of peak power corresponds exactly with DMSP observations [*Turman*, 1977, 1978]. We note that we have assumed that all events occur at nadir so that off-nadir range errors likely do exist. We also have not accounted for atmospheric extinction. The removal of these range and extinction errors would elevate the median value of peak power. We find that ~8% of our filtered events have peak powers $>10^{10}$ W, while only ~0.4% and ~0.004% have peak powers $>10^{11}$ W and $>10^{12}$ W respectively. We note that this occurrence frequency for detected events having peak amplitudes $>10^{12}$ W is 80 times greater than previously reported [*Turman*, 1977, 1978].

We can employ the pulse width observed by the PDD to acquire information concerning the optical depth of the intervening clouds, which serve to scatter the light emitted at the source. A comparison of the PDD-observed pulse width with those from optical lightning pulses observed from aircraft and ground-based instrumentation can reveal the additional path length traveled by a photon as a result of scattering. However, as can be seen in Figure 2 the pulse shapes observed by the PDD are not always amenable to an actual pulse-width calculation. Instead, we infer an “effective pulse width” based on the energy and peak irradiance of the observed pulse. This inference is based upon an assumption that the effective pulse widths are nominally much smaller than the PDD record length. To calculate the effective pulse width, we integrate an observed pulse through the 1.9-ms data window. We then normalize this representation of pulse energy by the reciprocal of the pulse’s peak irradiance. The resulting moment-of-energy parameter has units of time (seconds) and serves as our effective pulse width. It is the width of a rectangular pulse having as much energy as the observed pulse, but at an amplitude corresponding with only the peak irradiance.

Figure 4 illustrates the effect of cloud scattering on the observed effective duration of filtered optical pulses. A comparison of PDD effective pulse widths with other observations taken from above clouds [e.g., *Brook et al.*, 1980, 1985; *Goodman et al.*, 1988] shows relatively good agreement, with a slight bias in the median PDD-observed effective pulse widths toward larger values. When we compare our median effective pulse duration with those obtained below clouds [e.g., *Guo and Krider*, 1982; *MacKerras*, 1973], we can infer a conservative estimate on the amount of additional path length incurred by cloud scattering. Taking the median effective pulse width of 200 microseconds observed below clouds in Australia by *MacKerras* [1973], and comparing them with our median effective pulse width of 580 microseconds, we infer a median additional path length through clouds of approximately 100 kilometers at optical wavelengths. We emphasize that this inference is derived through the use of observations of lightning emissions, in which thick storm clouds are usually involved, and thus should not be taken to represent fair-weather cloud conditions. We suggest that this median value of additional path length represents a lower bound on the actual median path length through storm clouds, as observed by the PDD. The argument for this statement follows.

The distribution shown in Figure 4 includes the effective pulse widths obtained from optical pulses similar to the 3rd and 4th traces from the left in Figure 2. These traces result from the dead time incurred in re-arming the PDD (described above) and the immediate triggering on optical signals that have already peaked and are diminishing in amplitude. The effective pulse widths obtained from these types of triggers likely underestimate the actual effective pulse widths by not including the pre-peak portion of the signal in the integral. Thus, we would expect some fraction of the effective pulse widths shown in Figure 4 to shift right, to larger values. So, we expect the median pulse width to similarly shift right, translating to a shift in the median additional path length through clouds to larger values. No effort will be made here to account for this bias in Figure 4.

Figure 5 shows the distribution of source optical energy for optical lightning events observed by the PDD. The source energy was calculated by assuming that all pulses had widths less than ~2 milliseconds. The time-integrated irradiance was calculated for all filtered events and range-corrected by assuming all events occurred at nadir when the satellite altitude was 825 km. These calculations will generally provide a lower bound on the optical energy of the sources. This statement follows from two assumptions. The first assumption was that there was no extinction of the optical signal due to cloud reflection or absorption. The second assumption was that all events were located at nadir rather than at off-nadir angles where the range increases by as much as 30% for a given altitude. We point out that these calculations also suffer from the same problem as described for the pulse width calculations: that some event traces will not contain the pre-peak portion of the optical emission and will result in a smaller value of calculated energy. Nevertheless, we find the pseudo-range-corrected optical energies observed by the PDD to lie in the same range as independent observations made above and below clouds. *Guo and Krider* [1982] report the average peak optical power of 2.3×10^9 W for first return strokes in Florida storms observed from the ground with a silicon photodiode in the 0.4 to 1.1-micron band. *Guo and Krider* [1982] also report the average peak optical power of 4.8×10^8 W for subsequent return strokes. Using the median pulse width of 200 μ s for return strokes observed on the ground in Australia by *MacKerras* [1973], we infer the source optical energies for first return strokes and subsequent return strokes in Florida. We indicate these inferred source energies in Figure 6. We also indicate the average peak power of all return strokes observed in Arizona by *Krider* [1966] and the statistical variation of the peak power of CG strokes estimated by *Goodman et al.* [1988] from measurements at 777.4-nm at 20 km altitude.

Summary

We have presented examples of optical measurements of terrestrial lightning obtained from the PDD instrument onboard the FORTÉ satellite. The observations compare favorably with previous satellite- and aircraft-based measurements of optical lightning emissions. The median peak power observed by the PDD is about 1×10^9 W, consistent with observations made by *Turman* [1977] using data from a DMSP satellite. We do observe events having amplitudes $>10^{12}$ W, but they are rare in our data set (equivalent to ~400 in 10^7 events c.f. the estimate by *Turman* [1977] of 5 in 10^7 events). Although

we can observe peak powers lower than $8 \times 10^7 \text{W}$, we find that our false trigger floor limits us in a statistical study to events having powers greater than $\sim 2 \times 10^8 \text{W}$ and that only a relatively small percentage of events lie below this false trigger threshold in any case. The broadening of optical pulses by photon scattering within clouds serves as a useful diagnostic to assess the additional path length through lightning-producing clouds. We estimate the median additional path length to be approximately 100 km. Finally, we generally observe features in the optical pulses that we speculate to be indicative of stepped leader activity in CG strokes or channel branching. Should corroborating data support this speculation, and should these features lend themselves to a classification scheme, these data may allow for a global survey of CG and IC events.

References

Brook, M., R. Tennis, C. Rhodes, P. Krehbiel, B. Vonnegut and O.H. Vaughan, Simultaneous observations of lightning radiations from above and below clouds, *Geophys. Res. Lett.*, 7, 267, 1980.

Brook, M., C. Rhodes, O.H. Vaughan, R.E. Orville and B. Vonnegut, Nighttime observations of thunderstorm electrical activity from a high altitude plane, *J. Geophys. Res.*, 90, 6111, 1985.

Christian, H.J., R.J. Blakeslee and S.J. Goodman, The detection of lightning from geostationary orbit, *J. Geophys. Res.*, 94, 13329, 1989.

Goodman, S.J., H.J. Christian and W.D. Rust, A comparison of the optical pulse characteristics of intracloud and cloud-to-ground lightning as observed above clouds, *J. Appl. Met.*, 27, 1369, 1988.

Guo, C. and E.P. Krider, The optical and radiation field signatures produced by lightning return strokes, *J. Geophys. Res.*, 87, 8913, 1982.

Jacobson A.R., S.O. Knox, R.C. Franz, D.C. Enemark, FORTE observations of lightning radio-frequency signatures: Capabilities and basic results, submitted to *J. Geophys. Res.*, 1998.

Krider, E.P., Some photoelectric observations of lightning, *J. Geophys. Res.*, 71, 3095, 1966.

MacKerras, D., Photoelectric observations of the light emitted by lightning flashes, *J. Atmos. Terr. Phys.*, 35, 521, 1973.

Sparrow, J.G. and E.P. Ney, Lightning observations by satellite, *Nature*, 232, 540, 1971.

Turman, B.N., Detection of lightning superbolts, *J. Geophys. Res.*, 82, 2566, 1977.

Turman, B.N., Analysis of lightning data from the DMSP satellite, *ibid.*, 83, 5019, 1978.

Vonnegut, B., O.H. Vaughan and M. Brook, Photographs of Lightning from the Space Shuttle, *Bull. Amer. Met. Soc.*, 64, 150, 1983.

Vorpahl, J.A., J.G. Sparrow and E.P. Ney, Satellite observations of lightning, *Science*, 169, 860, 1970.

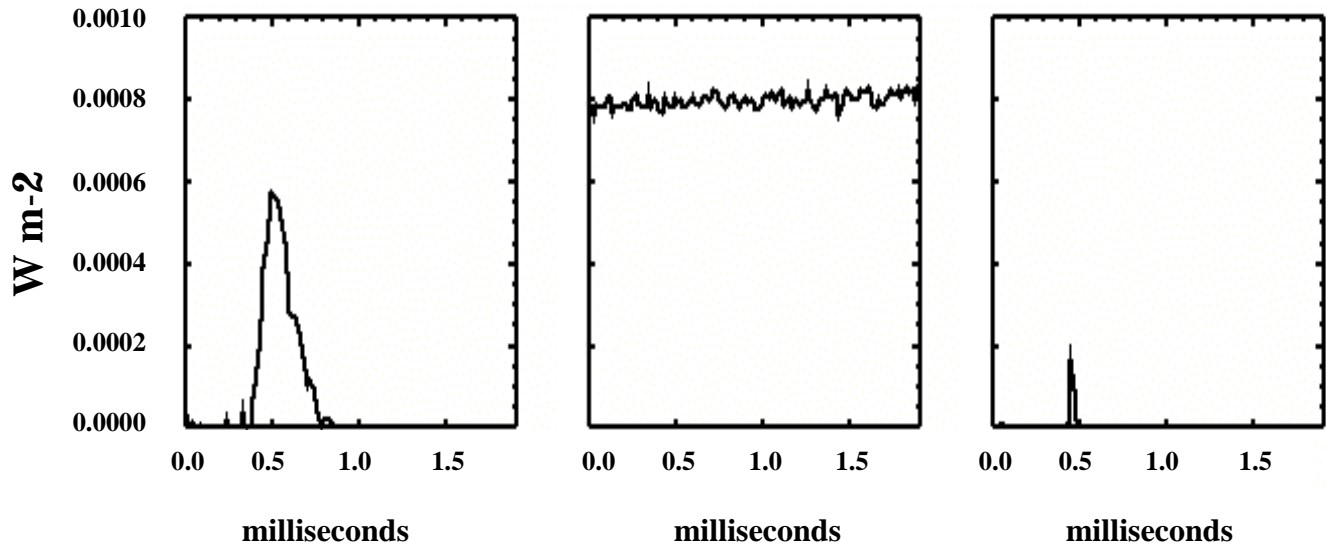


Figure 1. Examples of a lightning optical signature (left), noise (center) and a particle signature (right) as observed the PDD. The abscissa gives time in milliseconds and the full width of the time window is 1.9 ms. The ordinate gives the irradiance in watts per square meter.

**PDD Event Sequence, 8 October 1997, 08:37:55 UT
Central Pacific Ocean**

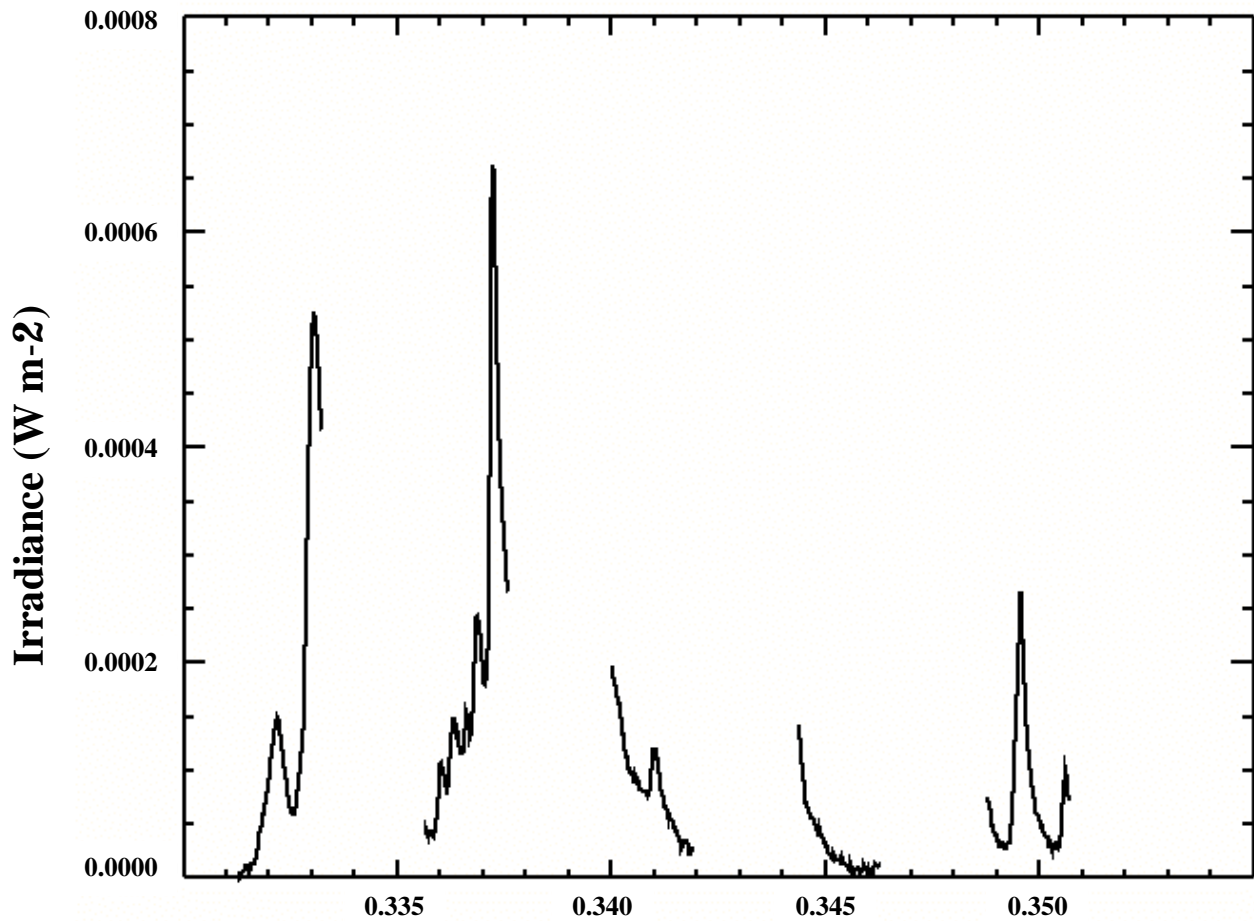


Figure 2. A sequence of lightning optical signatures observed over the central Pacific ocean on 8 October 1997 at 08:37:55 UT (22:37:55 Local Time). Abscissa gives time in fractional seconds from the last whole UT second. The ordinate gives irradiance in watts per square meter. cutoff is artificial and arises primarily from the imposition of the noise rejection criterion, although the events at the lowest amplitudes in the unfiltered distribution are typically removed by the imposition of the particle rejection criterion. We note that the left edge of the unfiltered distribution differs from the artificial cutoff by only a small amount in terms of absolute irradiance. If we assume that the trailing edges of both distributions have some physical basis, then a reasonable threshold to characterize a “false trigger floor” would be approximately $2.5 \times 10^{-5} \text{ Wm}^{-2}$.

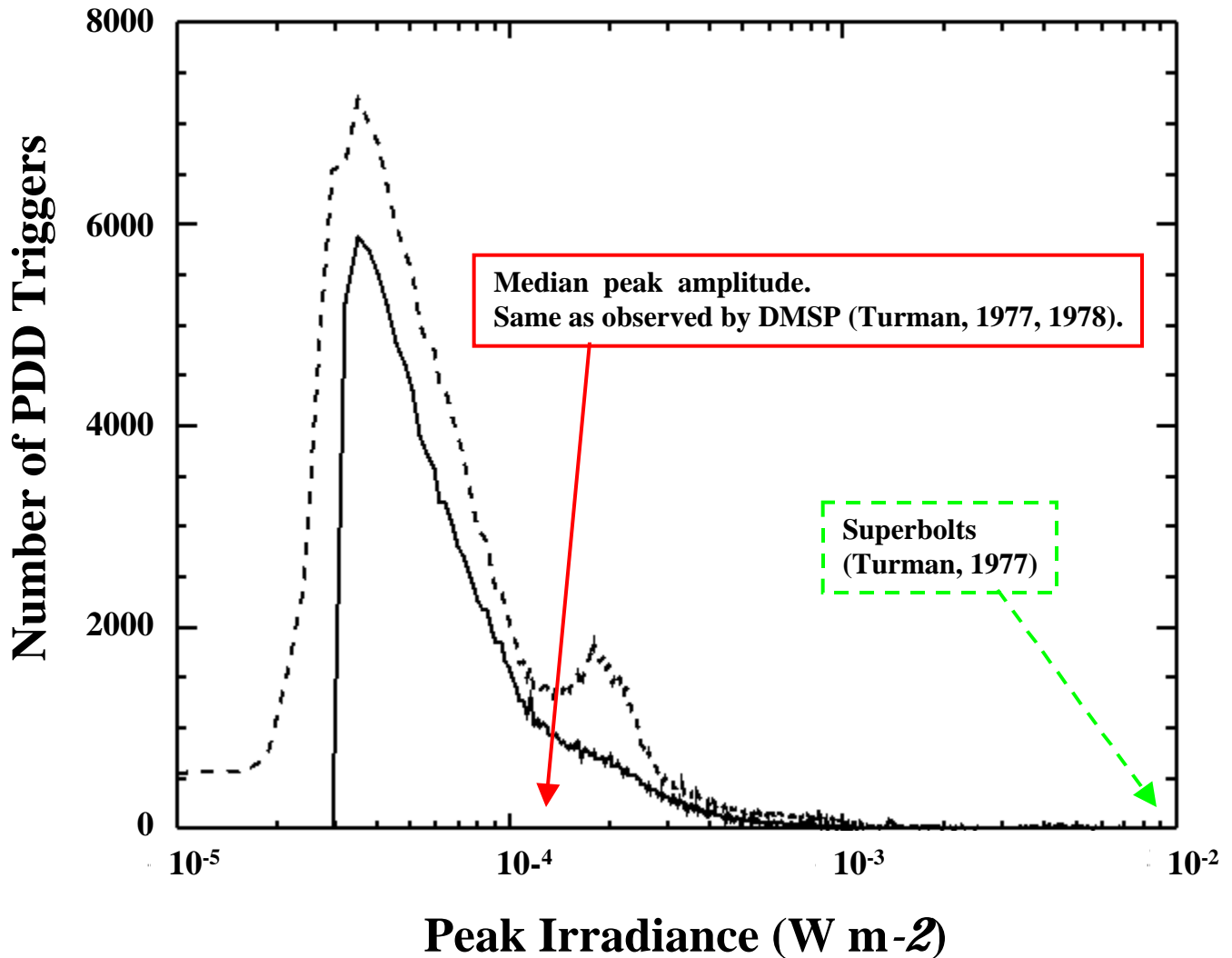


Figure 3. Occurrence distribution of peak irradiance for events observed during the first seven months of PDD operation. The abscissa gives irradiance in watts per square meter. The ordinate gives the number of triggers falling into each irradiance bin. The dashed curve represents all events, the solid curve represents only filtered events (see text for details). The approximate irradiance corresponding to the median peak power observed by *Turman* [1977, 1978] is indicated, as is the approximate irradiance for superbolt-class events. The plot window artificially truncates the distribution at both ends in deference to the most significant portion of the distribution.

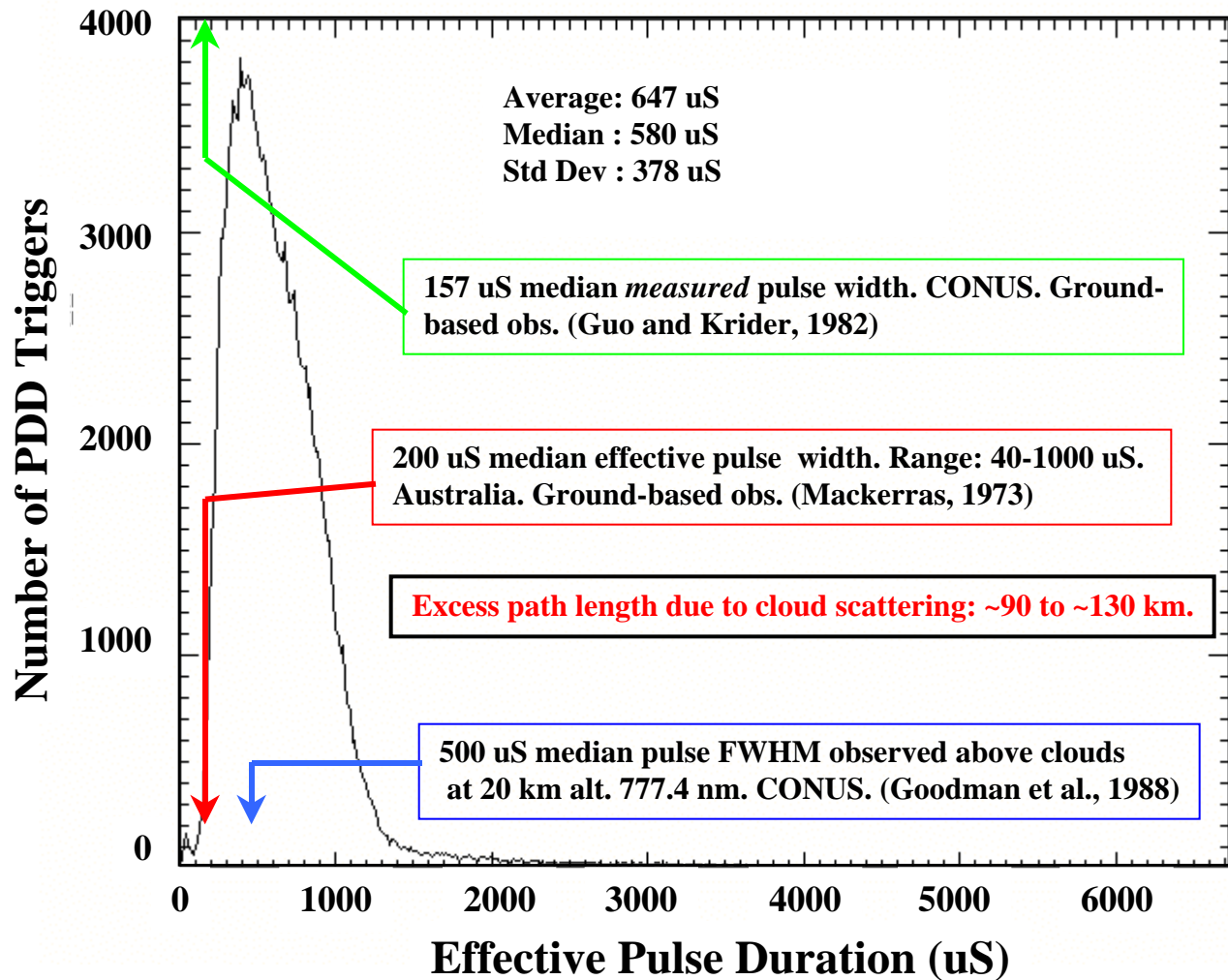


Figure 4. Occurrence distribution of the effective optical pulse widths observed during the first seven months of PDD operation for filtered events. The abscissa gives the effective pulse width in microseconds. The ordinate give the number of occurrences in each pulse width bin. The median effective pulse width is 580 microseconds, comparable to the pulse widths previously observed at 20-km. By comparing this pulse width to the median effective pulse width measured on the ground in Australia (200 microseconds), we infer an additional path length of approximately 100 km through the storm clouds associated with the lightning events.

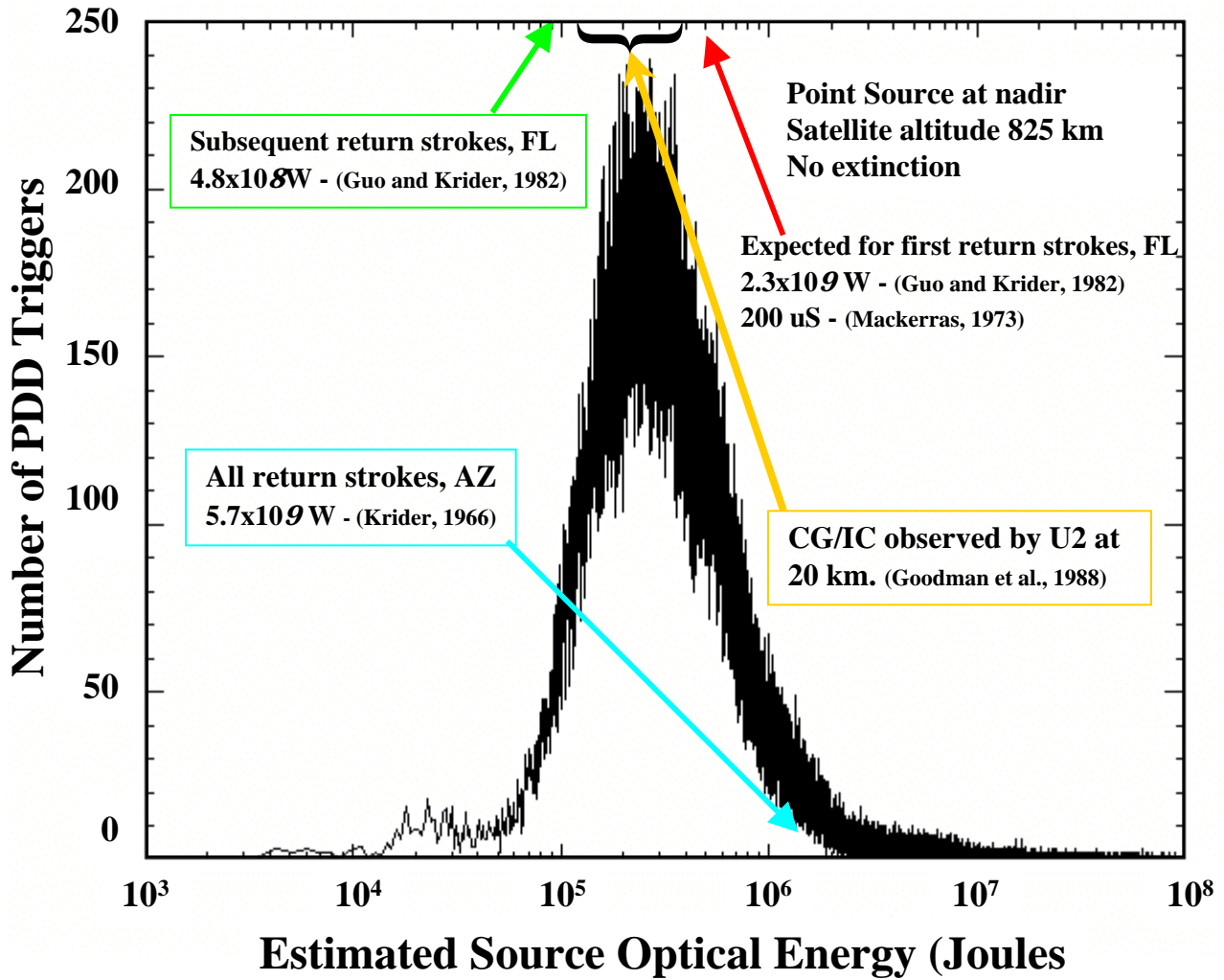


Figure 5. Occurrence distribution of the estimated lower bounds of source optical energies for the same population filtered events shown in Figure 4. The abscissa gives the source energy in joules. The ordinate gives the number of events in each energy bin. Our estimates of the source energy are comparable with previous observations.